Title: Non-necessary neural activity in the primate cortex

Authors: Sébastien Tremblay[1,†,§], Camille Testard[1,†,§], Jeanne Inchauspé[1,‡], Michael Petrides[1]

Affiliations:

[1]Montreal Neurological Institute, McGill University; Montréal, QC, Canada.

[†]Current affiliation: Department of Neuroscience, University of Pennsylvania; Philadelphia, PA, USA

[‡]Current affiliation: Department of Medicine, University of Oxford; Oxford, UK

[§]These authors contributed equally to this work

Abstract: When neurophysiologists record neural activity from the brain, they often conclude that neural tuning to task variables indicates a functional role of the brain area studied in task performance. However, it remains unknown how reliably such correlations indicate a functional role. To answer this question, we chronically recorded neural activity in the prefrontal cortex of monkeys during the performance of four cognitive tasks. Previous studies had demonstrated that only one of those tasks causally depends on the recorded area; the other three tasks are not impaired by lesions of this area. We found that the prevalence and strength of single neuron and ensemble tuning were equivalently high across all four tasks. This suggests that non-necessary cognitive signals are prevalent in the cerebral cortex of primates during task performance, challenging one of the fundamental assumptions of cognitive neurophysiology.

One-Sentence Summary: Tremblay, Testard and colleagues show that inferring a brain area's function from neural recordings during task performance is problematic.

Recording neural activity from awake behaving animals is a common approach to study the role of different brain areas in cognitive processing[1–3]. For example, neural activity correlating with decision variables during a task (e.g. value) may indicate that the recorded neurons play a key role in those decisions[4]. Using this inferential logic, various roles have been assigned to areas of the cerebral cortex of mammals, including humans[5–7]. This method, however, can only provide correlational evidence of the involvement of a brain area in a given cognitive process[8]. How reliable those correlations are at revealing a given brain area's functional role remains uncertain.

The inferential power of the neurophysiological approach is limited by the potential presence of "non-necessary" neural activity in the brain, that is, neural activity correlated with certain task variables that play no necessary role in the performance of that task (i.e. abolishing this activity does not impair task performance)[9]. The presence of such neural activity can mislead investigators when hypothesizing about the functional role of a brain area in health and disease[10,11]. Models based on such correlational evidence can lead to contradictory theories of brain function[12,13] and could identify ineffective therapeutic targets. Moreover, the number of proposed roles for each brain area inflates over time as more of these correlations are uncovered[14].

In the present study, we sought to investigate the prevalence of non-necessary signals in one intensely studied part of the primate brain: the prefrontal cortex (PFC). We focused on a brain area within the PFC with a defined role based on double dissociation studies in human and non-human primates. Area 8A of the primate PFC is known to be necessary for the conditional selection of visual stimuli based on instruction cues, as shown by a severe deficit following bilateral lesions to this area[15,16]. The same area plays no necessary role in other processes, such as visual discrimination and working memory, as shown by unaltered performance following complete, bilateral 8A lesions, but impaired performance following lesions to other neighboring cortical areas (i.e. double dissociation)[16–18].

Using chronic neural implants, we recorded simultaneously from neural populations in area 8A of the same monkeys during the performance of four different cognitive tasks (**Figure 1A, B**). Critically, based on earlier lesion studies, only one of the selected tasks causally depends on area 8A as shown by impaired performance after lesions to this area; performance on the other three tasks does not depend on area 8A (**Figure 1C**). We compared single neuron spiking activity across the four tasks using standard metrics widely used in the field to uncover the neural basis of cognition: single neuron tuning[19], persistent firing activity[20], and neural ensemble single-trial decoding[21]. We tested whether differential neural activity between tasks would reliably reflect the known functional involvement of this brain area.

Two macaque monkeys were trained on the following four tasks before the beginning of neural recording sessions: a conditional associative task (CAT), a visual discrimination task (VDT), a delayed match-to-sample task (DMS), and a spatial version of the delayed match-to-sample task (DMS-s). Only the CAT task is known to depend critically on brain area 8A; the other three tasks do not (**Figure 1C**). Behavioral performance was high across all four tasks and monkeys (>80%) and comparable across tasks (**Figure 2A**). Custom Utah arrays were used that fitted optimally within area 8A based on individual anatomy and vasculature (**Figure 1D**). We recorded simultaneously from an average of 166 single and multi-units in monkey K and 134 in monkey L in each session (40 sessions, 5 per monkey per task, total of 3335 units and 2688 units for monkey K and L, respectively). The number of recorded neural units was comparable across tasks for each monkey (**Figure 2B**).

We focused the analyses on a key epoch that is comparable across tasks: the delay epoch (see **Methods**). During that epoch, there are no stimuli on the screen and the monkey cannot prepare a motor response because of the randomization of target locations in the following epoch (except in the case of the DMS-s where motor responses can be planned). For these reasons, in the delay epoch the "cognitive" representations are dissociated from direct sensory and/or motor representations. In the cognitive neurophysiology field, functional roles of brain areas are typically inferred from the presence of cognitive representations during the delay[22].
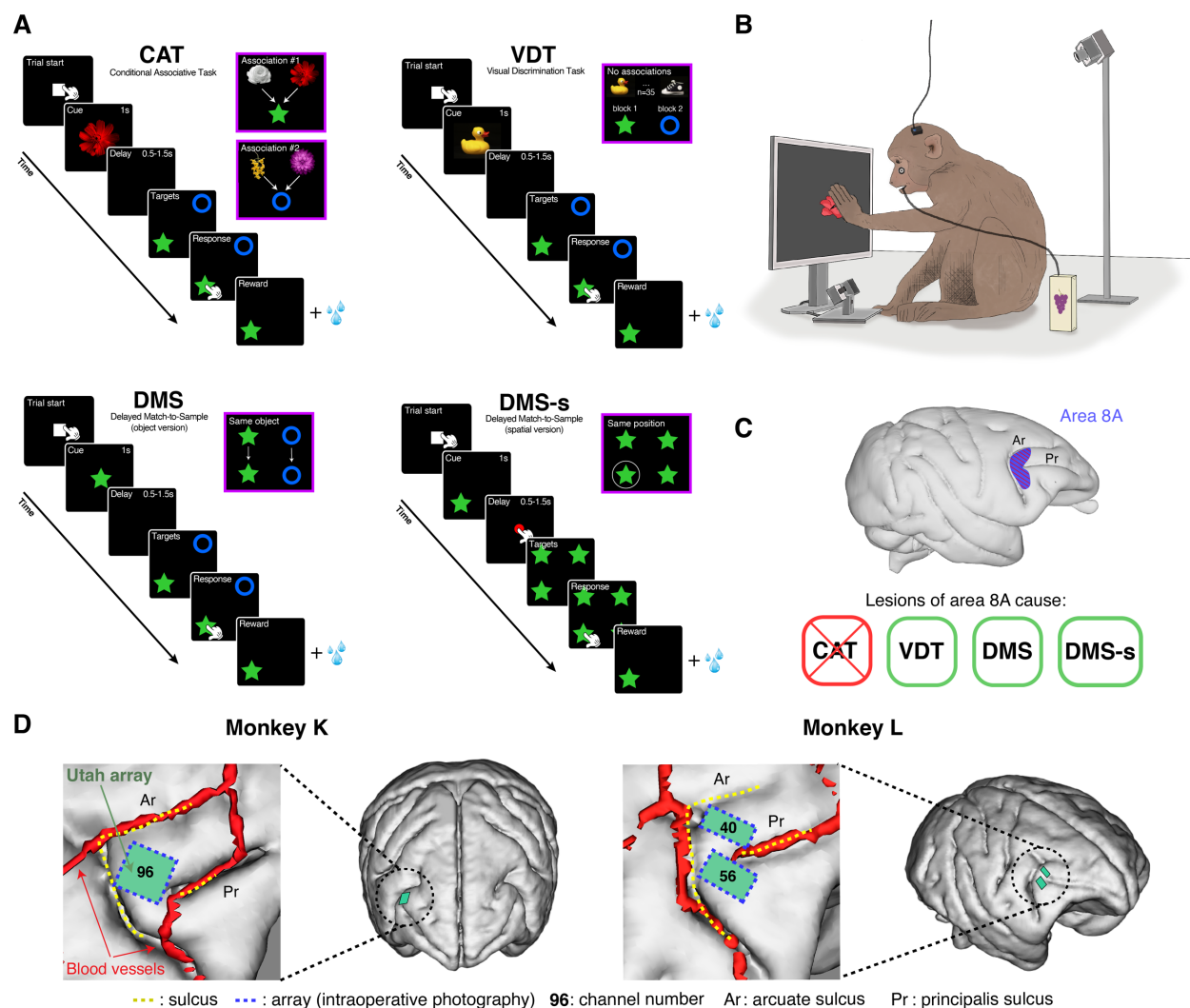

Fig. 1. Behavioral tasks, dissociation of function, and neural recordings. (**A**) Monkeys performed four different cognitive tasks on a touchscreen while neural activity was recorded through the same chronic implants. Each task had the same format and included a cue, delay, and response epoch. The CAT task required selecting the correct target based on the conditional relation of the visual cue to the targets. The VDT task required selecting the same target on every trial, regardless of the visual cue presented. The DMS task required selecting the target that was identical to the previously presented cue. The DMS-s task required selecting the target based on the position of the previously presented cue. In DMS-s, the delay was initiated after pushing a red circle at the center of the screen. This was to prevent the monkeys from leaving their hands at the cued position. (**B**) Depiction of the experimental setup. Monkeys were not head-restrained and were monitored through video cameras. (**C**) Results from previous lesion studies from our group showing that only CAT performance is affected by bilateral lesions to area 8A. Performance of VDT, DMS, and DMS-s is not. (**D**) Position of chronic Utah array implants within area 8A of both monkeys. Brain and vasculature reconstructed from MRI.
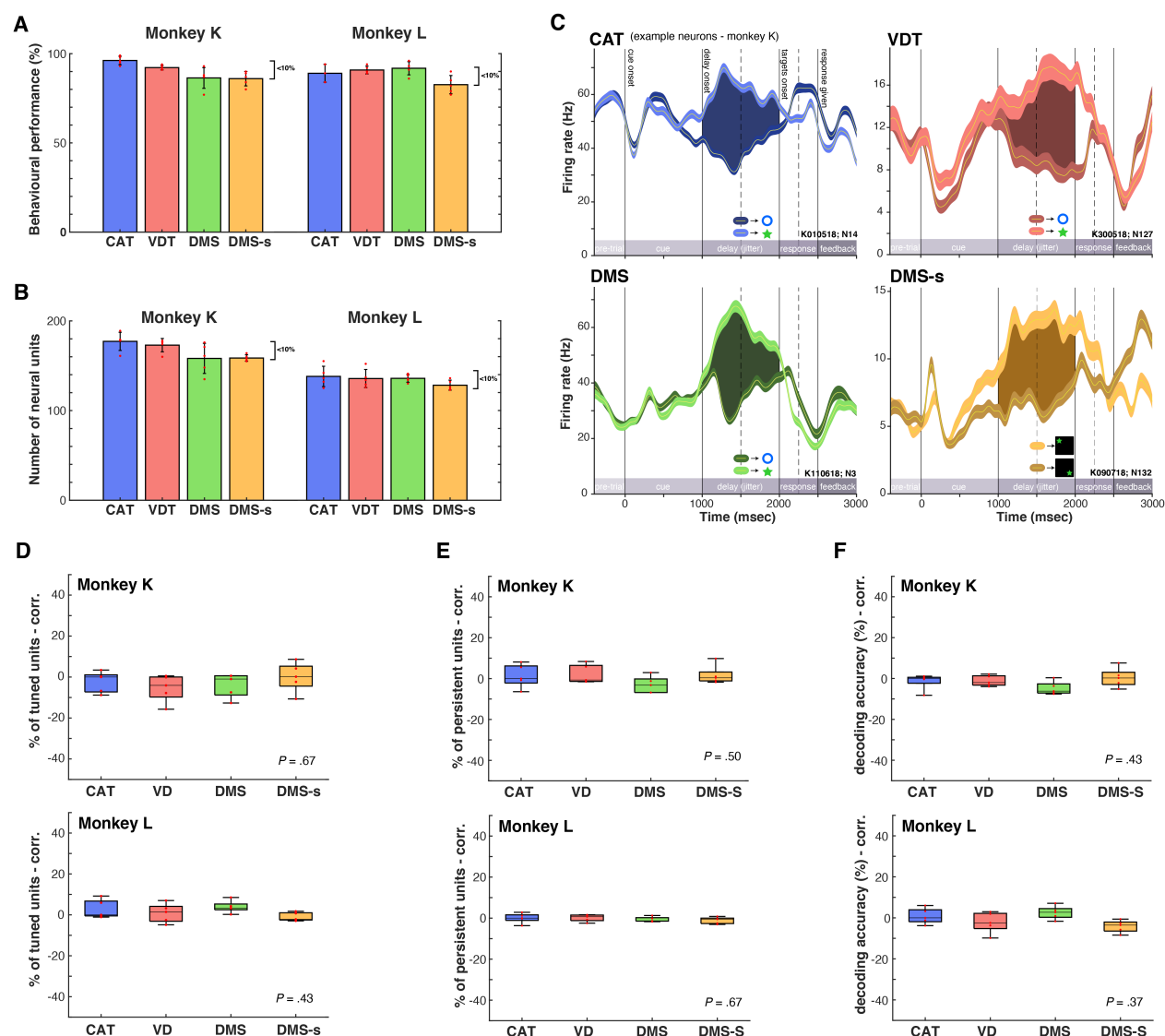
Fig. 2. Comparisons of behavioral performance and neural activity across the four tasks. (**A**) Behavioral performance of both monkeys on each of the four tasks. Average performance was comparable across tasks (all means fall within a 10% interval). Red dots indicate individual sessions. 5 sessions per task. (**B**) Number of neural units (single and multi-units) recorded simultaneously during each task. The average number of units recorded was similar across tasks for each monkey. (**C**) Example single neuron spiking activity during the performance of each task, averaged over trials, for monkey K. Trials are separated based on whether target 1 or target 2 needed to be selected on this trial. This selection depended on the cognitive task. Shaded area shows significant tuning during the delay epoch of each task, when no stimuli are on the screen. Error bars are SEM. (**D**) Proportion of neurons showing significant tuning during the delay, relative to CAT (CAT = 0), for each task. *P* values represent one way ANOVA comparing means of the four tasks, corrected for uninstructed movements (see **Methods** and **Supp. Fig 2**). (**E**) Proportion of persistent firing units, relative to CAT, for each task. *P* values as in (D). (**F**) Single-trial decoding accuracy of a support vector machine predicting target selection during the delay epoch, relative to CAT. *P* values as in (D). Box plots in (D-F) represent median and the 25th and 75th percentiles. *P*-values are FDR-corrected.

Because each task taps into a dissociable cognitive process (i.e. conditional visual selection, unconditional visual selection, working memory for object, and working memory for space in CAT, VDT, DMS and DMS-s, respectively; see **Methods**), neurons must encode different

cognitive representations to support behavioral performance. We tested whether neurons in area 8A encoded the representation required for CAT performance only, or whether they also encoded the ones required by the other tasks (which do not depend on area 8A). Surprisingly, we found evidence of single neuron tuning to the cognitive representation required by all four tasks in both monkeys (**Figure 2C** & **Figure S1**).

Although single neuron examples can be revealing, the field typically considers the proportion of all neurons recorded that exhibit similar tuning to support claims about function[23]. We thus compared the proportion of tuned neurons across all tasks relative to the CAT task. After correcting for task-aligned uninstructed movements that bias tuning[24,25] (see **Methods**), we found no difference in the proportion of tuned neurons across tasks in either monkey (**Figure 2D & Fig S2, S3, S4**). In all tasks, about 30% of neurons recorded during a session exhibited statistically significant tuning during the delay epoch (ANOVA, $P = .67$ and $P = .43$ for monkey K and L, respectively).

Another neural activity metric widely thought to represent cognitive processing is persistent firing activity during the delay[26] (although debated, see[27]). Thus, we tested whether differences would arise between tasks when the temporal persistence of neural tuning is compared. We used a conservative criterion for defining persistent activity: significant selectivity during at least 5 consecutive 100 msec bins during the delay ($P < .01$; minimal delay length = 500msec). Example neurons that would satisfy this criterion are displayed in **Figure 2C**. When quantifying the proportion of all neurons satisfying this criterion across the four tasks, we found no significant differences across tasks relative to CAT (**Figure 2E**, ANOVA, $P = .50$ and $P = .67$ for monkey K and L, respectively). Around 5% of neurons exhibited persistent activity during the delay, regardless of whether the task depends on area 8A (CAT), or not (VDT, DMS, & DMS-s).

Single neuron tuning and persistent selectivity metrics are based on average firing rates over trials. Although these metrics are informative, they ignore some important neural dynamics unfolding at the population level on a moment-by-moment basis[28]. As the field is developing an appreciation for those dynamic features, more investigators are focusing on single-trial analyses from simultaneously recorded neural ensembles[29]. A popular approach is to use decoding algorithms, such as support vector machines, to decode representations from ensemble activity on single trials[30,31]. Using this approach, we compared the decoding accuracy of cognitive representations across the four tasks using simultaneously recorded neural ensembles from area 8A. Again, our analyses revealed no difference in the single-trial decoding accuracy across tasks (**Figure 2F**, ANOVA, $P = .43$ and $P = .37$ for monkey K and L, respectively). All four cognitive representations were decoded with an average of 90% accuracy (SVM, k-fold = 5, see **Methods**).

Neural recordings are powerful approaches to investigate the neural correlates of cognitive processing. However, how reliable these correlates are at revealing the functional role of specific brain areas in the context of complex interacting neural circuits remains uncertain. Our results demonstrate that strong neural tuning was present during the delay epoch both at the single and neural ensemble levels, even in cases where this neural activity is known to not be necessary for task performance (i.e. lesion of these neurons do not affect task performance). This was true both when tuning is calculated using traditional 'average-over-trials' metrics and when using newer single-trial decoding methods. Taken in isolation, results from a single task could have led us to suggest incorrectly that area 8A "plays a role" in visual discrimination, or working memory.

It remains possible that differences in neural tuning across tasks occur at a different task epoch or require more sophisticated analytical approaches to be detected. We intentionally limited our

analyses to standard ones used in the field of cognitive neurophysiology: single neuron tuning and decoding of the upcoming choice during the delay epoch. Conclusions about the contribution of a brain area in a given cognitive process are typically based on those analyses[32,33]. However, our results suggest that such correlations between neural activity and task variables are not reliable indicators of function. We believe this is especially problematic for higher associative brain areas where functional roles are still unclear and undergoing intense investigation.

Why do we find neural signals that do not contribute to task performance (i.e. that are not necessary)? One potential explanation is that neurons are representing inputs the area needs to perform its specialized computation (e.g. visual or memory signals) even when the area is not necessary for current task demands. Another explanation is that these signals are simply feedback from other connected areas where the critical processing happens. In any case, without clear causal evidence establishing a framework within which these correlations can be interpreted, it is likely that investigators capture neural signals that may misrepresent the functional role of the brain area studied. This can fuel contradictions in the literature and slow progress in cognitive neuroscience. Based on the reported results, we recommend conducting neuro-correlational studies in primates only once the general function of a brain area has been elucidated through causal studies.

References and Notes

1. Goldman-Rakic, P. S. Cellular and circuit basis of working memory in prefrontal cortex of nonhuman primates. *Progress in brain research* 85, 325-35-discussion 335-6 (1990).

2. Newsome, W. T., Britten, K. H. & Movshon, J. A. Neuronal correlates of a perceptual decision. *Nature* 341, 52–54 (1989).

3. Xie, Y. *et al.* Geometry of sequence working memory in macaque prefrontal cortex. *Science* 375, 632–639 (2022).

4. Padoa-Schioppa, C. & Assad, J. A. Neurons in the orbitofrontal cortex encode economic value. *Nature* 441, 223–226 (2006).

5. Kable, J. W. & Glimcher, P. W. The neurobiology of decision: consensus and controversy. *Neuron* 63, 733–745 (2009).

6. Shadlen, M. N. & Kiani, R. Decision making as a window on cognition. *Neuron* 80, 791–806 (2013).

7. Chang, S. W. C. *et al.* Neuroethology of primate social behavior. *Proceedings of the National Academy of Sciences* 110 Suppl 2, 10387–10394 (2013).

8. Fellows, L. K. *et al.* Method matters: an empirical study of impact in cognitive neuroscience. *Journal of cognitive neuroscience* 17, 850–858 (2005).

9. Katz, L. N., Yates, J. L., Pillow, J. W. & Huk, A. C. Dissociated functional significance of decision-related activity in the primate dorsal stream. *Nature* 535, 285–288 (2016).

10. Wilson, C. R. E. *et al.* Prefrontal Markers and Cognitive Performance Are Dissociated during Progressive Dopamine Lesion. *Plos Biol* 14, e1002576 (2016).

11. Fellows, L. K. & Farah, M. J. Is anterior cingulate cortex necessary for cognitive control? *Brain* 128, 788–796 (2005).

12. Kolling, N., Behrens, T., Wittmann, M. K. & Rushworth, M. Multiple signals in anterior cingulate cortex. *Current Opinion in Neurobiology* 37, 36–43 (2016).

13. Hayden, B. Y. & Heilbronner, S. R. All that glitters is not reward signal. *Nature Neuroscience* 17, 1142–1144 (2014).

14. Stalnaker, T. A., Cooch, N. K. & Schoenbaum, G. What the orbitofrontal cortex does not do. *Nature Neuroscience* 18, 620–627 (2015).

15. Petrides, M. Deficits in non-spatial conditional associative learning after periarcuate lesions in the monkey. *Behavioural brain research* 16, 95–101 (1985).

16. Petrides, M. Conditional Learning and the Primate Frontal Cortex. in (ed. Ellen, P.) 91–108 (IRBN Press, 1987).

17. Petrides, M. Functional specialization within the dorsolateral frontal cortex for serial order memory. *Proceedings. Biological sciences / The Royal Society* 246, 299–306 (1991).

18. Petrides, M. Monitoring of selections of visual stimuli and the primate frontal cortex. *Proceedings. Biological sciences / The Royal Society* 246, 293–298 (1991).

19. Rainer, G., Asaad, W. F. & Miller, E. K. Selective representation of relevant information by neurons in the primate prefrontal cortex. *Nature* 393, 577–579 (1998).

20. Leavitt, M. L., Mendoza-Halliday, D. & Martinez-Trujillo, J. C. Sustained Activity Encoding Working Memories: Not Fully Distributed. *Trends in neurosciences* (2017) doi:10.1016/j.tins.2017.04.004.

21. Quiroga, R. Q. & Panzeri, S. Extracting information from neuronal populations: information theory and decoding approaches. *Nature Reviews Neuroscience* 10, 173–185 (2009).

22. Goldman-Rakic, P. S. Cellular basis of working memory. *Neuron* 14, 477–485 (1995).

23. Bruce, C. J. & Goldberg, M. E. Primate frontal eye fields. I. Single neurons discharging before saccades. *Journal of neurophysiology* 53, 603–635 (1985).

24. Musall, S., Kaufman, M. T., Juavinett, A. L., Gluf, S. & Churchland, A. K. Single-trial neural dynamics are dominated by richly varied movements. *Nature Neuroscience* 1–16 (2019).

25. Tremblay, S., Testard, C., DiTullio, R. W., Inchauspe, J. & Petrides, M. Neural cognitive signals during spontaneous movements in the macaque. (2022) doi:10.1101/2022.09.05.506681.

26. Constantinidis, C. *et al.* Persistent Spiking Activity Underlies Working Memory. *J Neurosci* 38, 7020–7028 (2018).

27. Lundqvist, M., Herman, P. & Miller, E. K. Working Memory: Delay Activity, Yes! Persistent Activity? Maybe Not. *J Neurosci* 38, 7013–7019 (2018).

28. Latimer, K. W., Yates, J. L., Meister, M. L. R., Huk, A. C. & Pillow, J. W. Single-trial spike trains in parietal cortex reveal discrete steps during decision-making. *Science (New York, NY)* 349, 184–187 (2015).

29. Rich, E. L. & Wallis, J. D. Decoding subjective decisions from orbitofrontal cortex. *Nature Neuroscience* (2016) doi:10.1038/nn.4320.

30. Tremblay, S., Pieper, F., Sachs, A. & Martinez-Trujillo, J. Attentional filtering of visual information by neuronal ensembles in the primate lateral prefrontal cortex. *Neuron* 85, 202–215 (2015).

31. Minxha, J., Adolphs, R., Fusi, S., Mamelak, A. N. & Rutishauser, U. Flexible recruitment of memory-based choice representations by the human medial frontal cortex. *Science* 368, eaba3313 (2020).

32. Huk, A. C., Katz, L. N. & Yates, J. L. The Role of the Lateral Intraparietal Area in (the Study of) Decision Making. *Annual review of neuroscience* 40, 349–372 (2017).

33. Moore, T. & Zirnsak, M. Neural mechanisms of selective visual attention. *Annual review of psychology* 68, 47–72 (2017).

34. Petrides, M. Lateral prefrontal cortex: architectonic and functional organization. *Philosophical Transactions of the Royal Society of London. Series B: Biological Sciences* 360, 781–795 (2005).

35. Mathis, A. *et al.* DeepLabCut: markerless pose estimation of user-defined body parts with deep learning. *Nature Neuroscience* 1–12 (2018) doi:10.1038/s41593-018-0209-y.

36. Nath, T. *et al.* Using DeepLabCut for 3D markerless pose estimation across species and behaviors. *Nat Protoc* 14, 2152–2176 (2019).

Acknowledgments

have no competing interests. **Data and materials availability:** The datasets generated and analyzed during the current study are available from the corresponding author on reasonable request.

Supplementary Materials and Methods

Subjects

Two adult male monkeys (cynomolgus monkeys, monkey K: 7 kg, monkey L: 7 kg) participated in the experiments. All procedures complied with the Canadian Council of Animal Care and the Montreal Neurological Institute animal care committee. Over the course of a testing session (once a day), the monkeys would receive their daily amount of fluids consisting of water-diluted fruit juice for correctly performing the task. In addition, the monkeys would receive daily fresh fruits and vegetables at the end of each recording session. Each session lasted on average one hour, and no more than 1.5 hour. The physical and mental health of the monkeys was assessed daily by veterinary and laboratory staff throughout the course of the experiment. No animals were sacrificed for the purpose of this study.

Surgical procedures

Surgical plans were prepared with the help of brain MR images obtained on a Siemens 3T scanner (TIM TRIO, Montreal Neurological Institute). T1-weighted images (MP-RAGE) with and without gadolinium enhancement (Gadovist®, Bayer, Germany) were obtained to reconstruct the 3D cortical surface and cerebral vasculature of the brains (Brainsight Vet 2.4, Rogue Research, Canada; see **Fig. 1D**). Custom Utah arrays (Blackrock Microsystems, UT) were designed on the basis of each monkey's neuroanatomy in order to cover optimally the region of interest while avoiding major blood vessels. All surgical operations were carried out under isoflurane general anesthesia and under strict sterile conditions with the help of experienced veterinary staff continuously monitoring vital signs. The animals' head was positioned in a stereotaxic frame (Kopf Instruments, CA) and a midline skin incision was made to expose the dorsal aspect of the skull. The temporalis muscles were retracted ventrally and a square-shaped craniotomy (1.5 x 1.5cm) was made in the fronto-lateral bone based on MRI coordinates using a dental drill equipped with a diamond round-cutting burr (Horico, Germany). The dura-mater was exposed and a dural flap was performed extending ventrally. Direct visualization of cortical landmarks (i.e. the arcuate and principalis sulci) enabled identification of the pre-arcuate convexity where cytoarchitectonic area 8A of the prefrontal cortex lies in the macaque brain[34]. The array(s) were positioned over the region of interest and implanted using a pneumatic inserter held by a flexible surgical arm. The dural flap was closed with 5-0 Vycril sutures and a layer of dura regeneration matrix (Durepair, Medtronic, MN) was laid over the reconstructed flap. The bone flap was thinned with a drill and replaced over the craniotomy and secured to the skull with low-profile titanium plates and screws (DePuy Synthes, IN). The Cereport connector was secured caudally to the skull opening using eight 1.5mm diameter titanium screws with a length determined by the skull thickness as measured by pre-operative MRI. The two reference wires were inserted in between the dura and the cortex and the exposed portion of those wires and of the array wire bundle were coated with a thin layer of Quick-Sil (WPI, FL) or Geristore (Denmat, CA). The muscle, fascia and skin were closed in anatomical layers with absorbable 3-0 Vycril sutures and the Cereport connector was allowed to protrude through a small opening in the skin. The monkeys were allowed to recover for two weeks

before the first recording session. No headposts were implanted in this study and no acrylic or dental cement was used in surgeries.

Behavioral tasks

In the current study, the monkeys were trained to sit in primate chairs that did not restrict their head or arm movements. The front panel of the chair was removed allowing the monkeys to reach outside the chair with their arms. The primate chair did not impose head movement restrictions, allowing the monkeys to turn around in the chair and look in any direction (360°). The monkeys were positioned in front of a 19-inch touchscreen (ELO touch 1937l, Accutouch, CA) connected to a behavioral control computer running MonkeyLogic 2.0 (version 47, NIMH, Hwang et al. 2019) on a Windows 7 PC. The chair was positioned 7 inches from the touchscreen, such that the monkeys could reach easily at all locations on the screen. At this distance, the screen occupied 86.4 degrees of visual angle horizontally and 73.7 degrees of visual angle vertically. The two monkeys were trained on four different computerized cognitive tasks: 1) conditional association task (CAT), 2) visual discrimination task (VDT), 3) delayed match-to-sample task (DMS), and 4) spatial DMS task (DMS-s). The four tasks were performed while recording from the same neural implants over a timespan of 4 months for monkey K, and 3 months for monkey L.

CAT

The CAT task is a computerized adaptation of the conditional association task used in Petrides et al.[15,16]. This task taps into the ability of subjects to select visual objects in their environment based on instruction cues that change from trial to trial. In this earlier study, monkeys with bilateral lesions of prefrontal area 8A (the area targeted in the current study) exhibited severe impairments on this task, while sparring cognitive performance on other equally difficult tasks, such as working memory tasks. A trial was initiated by touching a white square appearing at the center of the touchscreen. Following the touch, one out of four possible visual instruction cues appeared on the screen for 1 second. After cue presentation, a delay period of random duration (0.5-1.5 sec) followed. After the delay, two targets appeared randomly at 8 possible locations (stimuli always opposite to each other). The monkeys received a reward if they touched the correct target associated with the cue presented earlier in the trial. Upon selection of the correct target, the untouched target disappeared to give feedback on what target was selected, and a squirt of juice was delivered through a metal straw (Crist Instrument, MD). Before the beginning of this experiment and over the course of multiple training sessions, the monkeys had learned 36 arbitrary cue-target associations, always using the same two targets (a blue circle and a green star), until a threshold of 80% accuracy was reached. In any given recording session (one session per day), 4 cues were selected (2 associated with the circle, 2 associated with the star) and were interleaved in a block design, whereby a first pair of cues (1 associated with each target) was presented for half the session, and a second pair for the other half of the session. Having two cues associated with each target option permitted dissociation of tuning for the cue vs tuning for the association. Behavioral performance at the task was calculated using a hit rate (correct trials / (correct trials + error trials)).

VDT

The VDT task is a computerized version of the visual discrimination task used in Petrides et al.[15,16]. This task taps into a subject's ability to select consistently a visual object in the environment regardless of contextual cues. Bilateral lesions to area 8A had no effect on VDT performance. In this task, the trial structure is the same as in the CAT task (1 sec cue, 500:1500 msec delay). The only difference is that the cues presented were not associated with the targets. Thus, the monkeys did not need to select a particular visual target based on the instructional cues presented to perform accurately, but rather had to choose the same target on every trial, regardless of the cue presented. On every trial, a cue was randomly selected from a bank of 35 cues. This large number of cues prevented monkeys from forming false associations between cues and targets, as was previously observed with a smaller set of 4 random cues (data not shown). To ensure the monkeys selected each target (circle and star) an equal number of times, each session had a block design, whereby the first half of the trials required selection of the circle target, and the second half required selection of the star target. This order was interleaved across sessions. Monkeys quickly learned which target to select in each block through trial and error.

DMS

The DMS task is a computerized version of the standard delayed match-to-sample task used in various lesion studies. This task taps into a subject's ability to remember an object item over time in order to guide a decision after a delay. It is typically considered a "working memory" task in the neurophysiology literature[26]. The DMS task had the same trials structure as the CAT and VDT task. A trial was initiated by pressing a white square at the center of the screen. After the touch, one out of two visual stimuli (circle or star stimuli) were presented at the center of the screen for 1 sec. Following a delay period of 500:1500 msec, two targets (star and circle) appeared randomly at 8 possible locations. The monkey was rewarded for selecting the target that was identical to the cue presented earlier.

DMS-s

The spatial DMS task is a spatial version of the delayed match-to-sample task. This task taps into a subject's ability to remember a spatial location in the environment in order to guide a decision after a delay. It is typically considered a "working memory" task in the neurophysiology literature. This task has the same trial structure as the CAT, VDT, and DMS tasks. First, a visual stimulus appears at one out of 4 possible locations on the screen for 1 sec. Following a delay period of 500:1500 msec, four targets appeared at each one of the four possible cue locations. The monkey was rewarded for selecting the target at the location that was cued earlier in the trial. To prevent the monkeys from simply leaving their hand at the cued location during the delay epoch (which would remove the memory component of this task), they had to place their hand back on a red dot at the center of the screen after cue offset to start the delay epoch.

Behavioral and video monitoring

Movements explain a large portion of the neural variance in this brain area and uninstructed movements aligned with task variables can bias estimates of neural tuning[24,25]. To account for this potential confound, we tracked head, eyes and body movements during task performance (**Fig. S2, S3**). All behavioral monitoring devices were synchronized to the master clock of the neural recording system. All touchscreen touches by the monkeys were recorded by MonkeyLogic and

marked as discrete events. In addition, we used a head-free eye tracking system to monitor eye position, pupil size, and head position (in 3D) with a 500 Hz temporal resolution (Eyelink 1000, Remote version, SR Research, Canada). This was achieved with the help a small sticker put on the monkeys' right cheek at the beginning of each session (see **Fig. S2a**). This eye tracking signal was lost when the monkeys made very large head movements (e.g. turning 180° in the chair) bringing the sticker out of the sight of the camera. Additionally, we video-recorded the body movements of the monkeys using a video camera installed on top of the primate chair (IDS UI-3240ML-C-HQ, 30 fps, Germany; **Fig. S2a**).

Using video data, we measured potential biases in eyes, head or body movements that correlated with the animals' decision on every trial (i.e. selecting the star or the circle target). We calculated the trial-averaged positions during the delay epoch, separating trials per target selected (e.g. star or circle). The distance between the average positions for star-selected and circle-selected trials is referred to as "bias" and indicate the difference in uninstructed movements made as a function of the decision taken during the delay (see **Fig. S2c,d**). Those movement biases correlated strongly with neural tuning, persistent activity and decoding accuracy in monkey K (see **Fig. S3**) We regressed out those spatial biases from our neural metrics comparisons across tasks to control for the effect of those task-aligned movements on tuning estimates (see details below).

Video tracking analyses

Using the data from the video camera attached to the primate chair, we computed the motion energy for the arms and head during performance of the task. The arms and head were parsed using manually drawn regions of interests (ROI) in the Motion Energy Analysis software (MEA v4.10, F. Ramseyer 2019, https://osf.io/gkzs3/). Motion energy was computed as the number of pixels that "change" value within the ROI on a frame-by-frame basis. A "change" was defined based on a threshold crossing operation on the pixel color change to eliminate video noise (threshold = 14 a.u.).

For body movements tracking we used DeepLabCut (version 2.2)[35,36]. Specifically, we labeled 200 frames taken from 3 videos/animals (then 95% was used for training) for the following key points: right hand, left hand, eyebrow, nose, tail. The tail and left hand were visible only for monkey L and K, respectively. We used a ResNet-50-based neural network with default parameters for 150,000 training iterations. We validated with 10 number of shuffles, and found the test error was: 6 pixels, train: 307,200 pixels (image size was 640 by 480). We then used a p-cutoff of 0.8 to condition the X,Y coordinates for future analysis. This network was then used to analyze videos from similar experimental settings and identify coordinates of all key points on a frame-by-frame basis (30 frames per second).

Neural recordings and spike detection

The neural data from the chronically implanted Utah arrays were recorded using a Cereplex Direct 96-channel neural recording system (Blackrock Microsystems, UT). The raw signal was bandpass filtered (0.3Hz to 7.5KHz) and digitized (16 bits) at 30,000 samples per second by a Cereplex E digital headstage installed on the Cereport connector of the Utah array. The digitized signal was routed from the headstage to the recording computer (PC, Windows 7) using a long, flexible micro-HDMI cable that did not impede the movements of the monkeys. For each channel, neural action potentials (or "spikes") were detected online based on a channel-specific voltage threshold equal

to 4 times the root mean square of the noise amplitude (Central Suite software, Blackrock Microsystems). The waveforms and timestamps of each spikes were saved to disk and transferred to Offline Sorter (version 2.8.8, Plexon Inc., TX) for manual sorting of spike waveforms. Well-isolated single units as well as multi-unit clusters were classified on each channel and saved for later analyses in Matlab (MathWorks, MA). On average, we recorded from 166 (SD 13.1) units (including single and multiunits) from Monkey K on each session and 134 (SD 8.5) from monkey L, or a total of 3335 units in K and 2688 units in L. We made no assumptions as to whether recorded units were the same or different ones from session to session. The number of recorded neurons was similar across tasks (**Figure 2B**).

Single neuron selectivity

Each task taps into a dissociable cognitive process, as detailed above. The firing rate of neurons can exhibit tuning/selectivity for the cognitive representation required by each task (i.e. conditional visual selection, unconditional visual selection, working memory for object, and working memory for space for CAT, VDT, DMS and DMS-s, respectively). The selectivity of each neural unit (single or multi-unit) was assessed during the delay period using a 500msec time interval [delay start +100msec: delay start +600msec]. During this time interval, the number of action potentials was counted for each trial. Trials were separated based on whether the option 1 (e.g. star) or the option 2 (e.g. circle) was the correct answer. For the DMS-s task, there were initially four options (i.e., positions) rather than two. We therefore pooled trials into two categories: right hemifield vs left hemifield to have comparable number of trials per category with other tasks. Average firing rates over trials for each option was compared using an ANOVA with $P < .01$, uncorrected. Because the number of trials can influence the probability of a statistically significant result (larger N leads to lower P values), we randomly subsampled trials for each session to the minimum number of trials obtained in all session (87 trials per condition for monkey K, 133 for monkey L). This approach ensured that the number of neurons crossing the statistical threshold could be compared across tasks without statistical power biases.

Common epoch across tasks: the delay epoch

Our analyses are focused on the delay epoch where no visual stimuli are on the screen and the monkeys cannot prepare a motor action (targets' locations are randomly selected during the target epoch, see **Figure 1**). Our reasons for focusing on this task epoch are two-fold. First, the delay epoch is the most common epoch analyzed by cognitive neurophysiologists in order to dissociate sensorimotor representations from "cognitive" representations. Second, it is the only epoch that is truly comparable across the four tasks. The cue epoch has different number and types of cues across tasks, making it impossible to compare tuning on equal grounds (CAT: 4 cues; VDT: 32 cues; DMS: 2 cues; DMS-s: 4 cues). It is also impossible to dissociate cue encoding from target encoding in a comparable manner, since the association between cues and targets is varied across tasks (1:1 in DMS, 4:2 in CAT, 32:0 in VDT).

Correction for movement biases

As demonstrated previously, a large part of the neural variance is explained by uninstructed movements in task-performing mice[24] and monkeys[25]. Since the amount of uninstructed movements varied across tasks (**Fig. S3**), to compare neural tuning, persistent activity, and

13

ensemble decoding accuracy consistently, we needed to remove the neural variance explained by movements. To do so, we ran a multilinear regression with either % tuned units, % persistent activity units, or % decoding accuracy as the dependent variable (one value per session). The independent variables were the trial-averaged uninstructed movements biases from the eyes, the cheek, the right hand, the left hand, the tail, the nose, the eyebrow, as well as the mean motion energy from the head and arms. A movement bias was defined as the mean difference between the motor effector's position (or energy) across the two target conditions during the delay epoch. The movement-controlled residuals from this multilinear regression were then used to compare tuning, persistent activity, or decoding accuracy across tasks using ANOVAs.

Proportion of tuned neurons

We computed the proportion of tuned neurons for each session as: (N tuned neurons / N neurons recorded). Because the proportion of tuned neurons is correlated with the presence of uninstructed movements aligned with task variables, we regressed out movement biases. This approach allows us to compare proportions of tuned neurons across tasks controlling for varying amounts of task-aligned uninstructed movements. Because the absolute value of these residuals is undefined, we presented values as relative to the CAT task, which we aligned with 0 on the Y-axis in **Fig 2**. Results in **Fig. 2D-F** are therefore presented relative to the reference task, CAT. Uncorrected estimates are presented in **Fig. S4**.
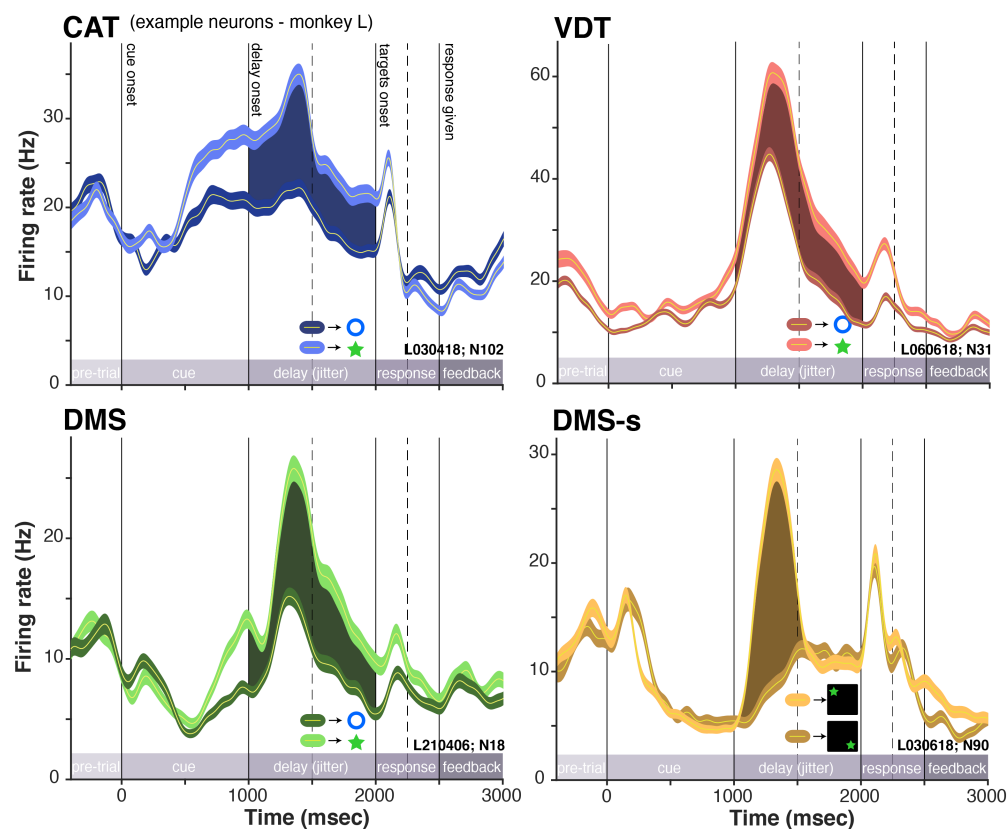
Persistent firing activity

Persistent firing activity was defined as statistically significant selectivity for at least 5 consecutive 100 msec time bins during the delay epoch ($P < .01$). Single unit selectivity as defined above. This allowed to detect units that had a relatively persistent firing rate in favor of one of the two options during the delay. The proportion of "persistent units" was compared across tasks using an ANOVA, following the same correction for uninstructed movements detailed above.
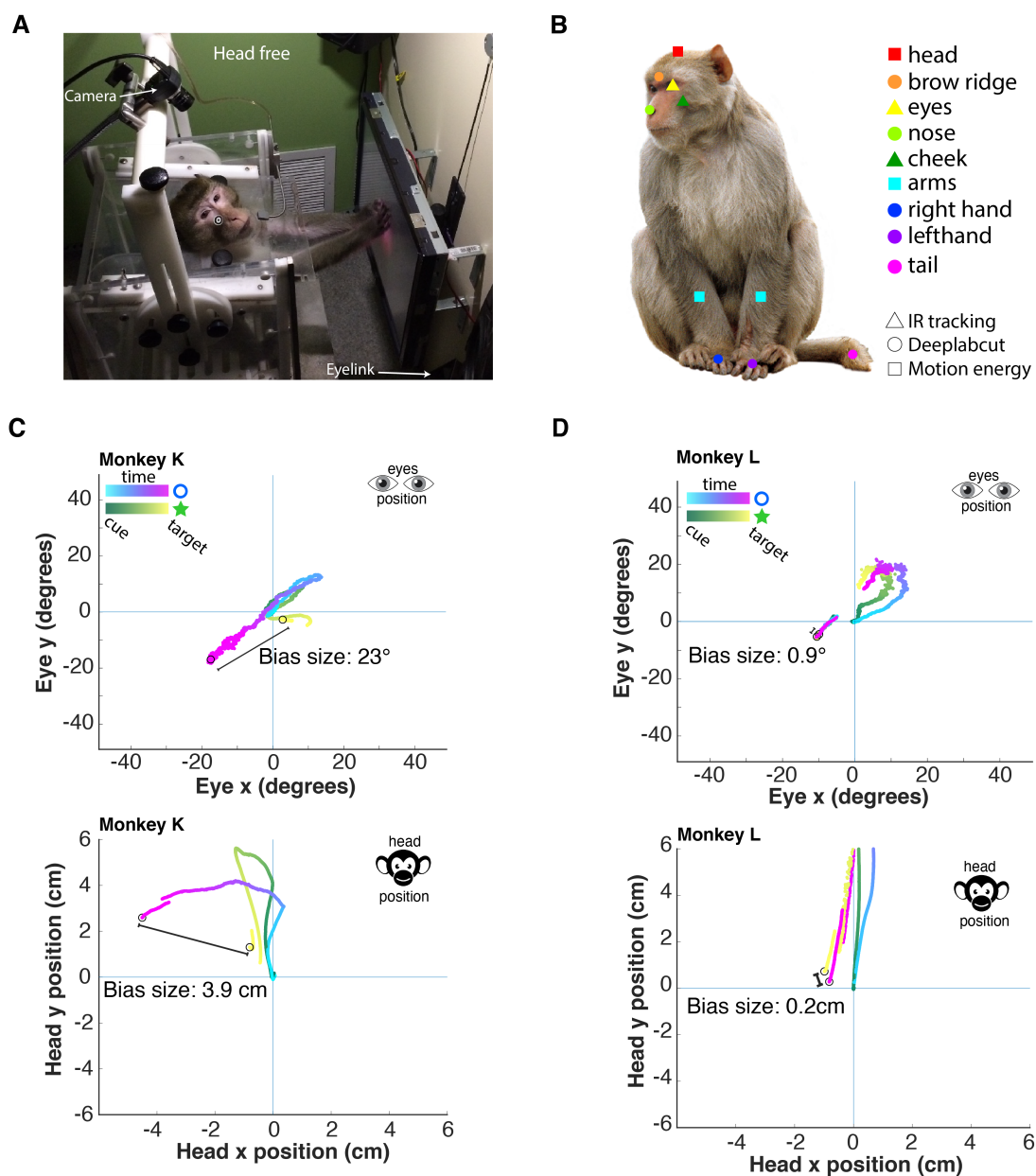
Decoding analyses

We ran decoding analyses using a machine-learning algorithm to estimate the amount of information contained in the neural firing code during the delay [delay start +100 msec : delay start +600msec]. In those analyses, we used a support vector machine (SVM) with an RBF kernel and 5-fold cross-validation. For each SVM, we only included simultaneously recorded units, hereby named "neural ensembles", to get a more realistic estimate of information content on a msec time resolution and to better account for confounding factors that can affect coding, such as noise correlations. For each cross-validation fold, a non-overlapping training and testing sets of trials were defined, and the accuracy of the trained model was calculated based on the number of correct predictions on the testing set (correct predictions / all predictions). The number of trials per class (2 classes, one for each target option) was balanced using random sampling so each class had the same number of observations as the smallest class. To account for the random sampling process, we ran 30 iterations of each SVM and computed the mean decoding accuracy across those iterations. Chance performance of the decoder was obtained by randomly permuting the labels (shuffled control) before training and following the same analysis procedure. The decoding accuracy for each session was compared across tasks using an ANOVA, following the same correction for uninstructed movements detailed above.
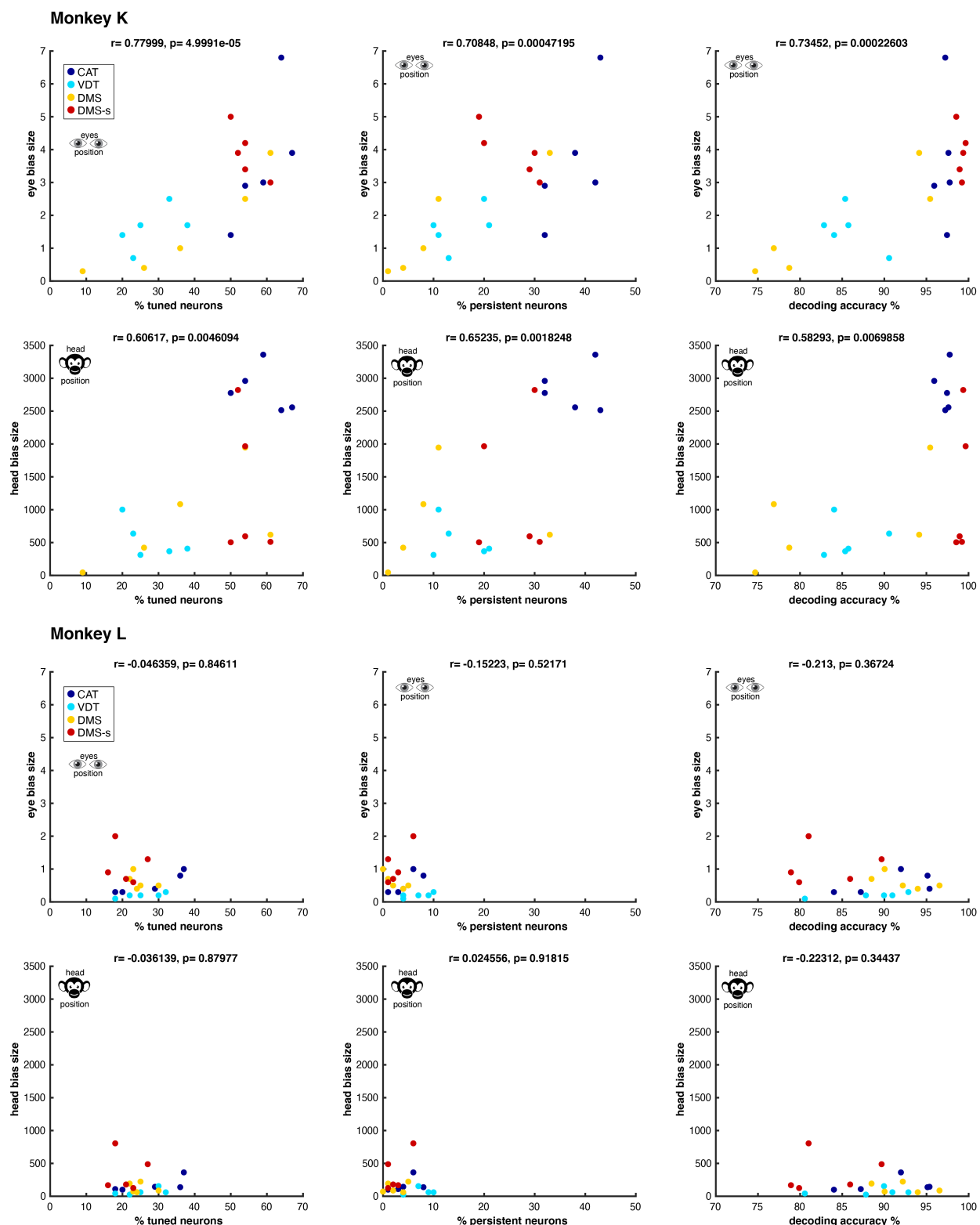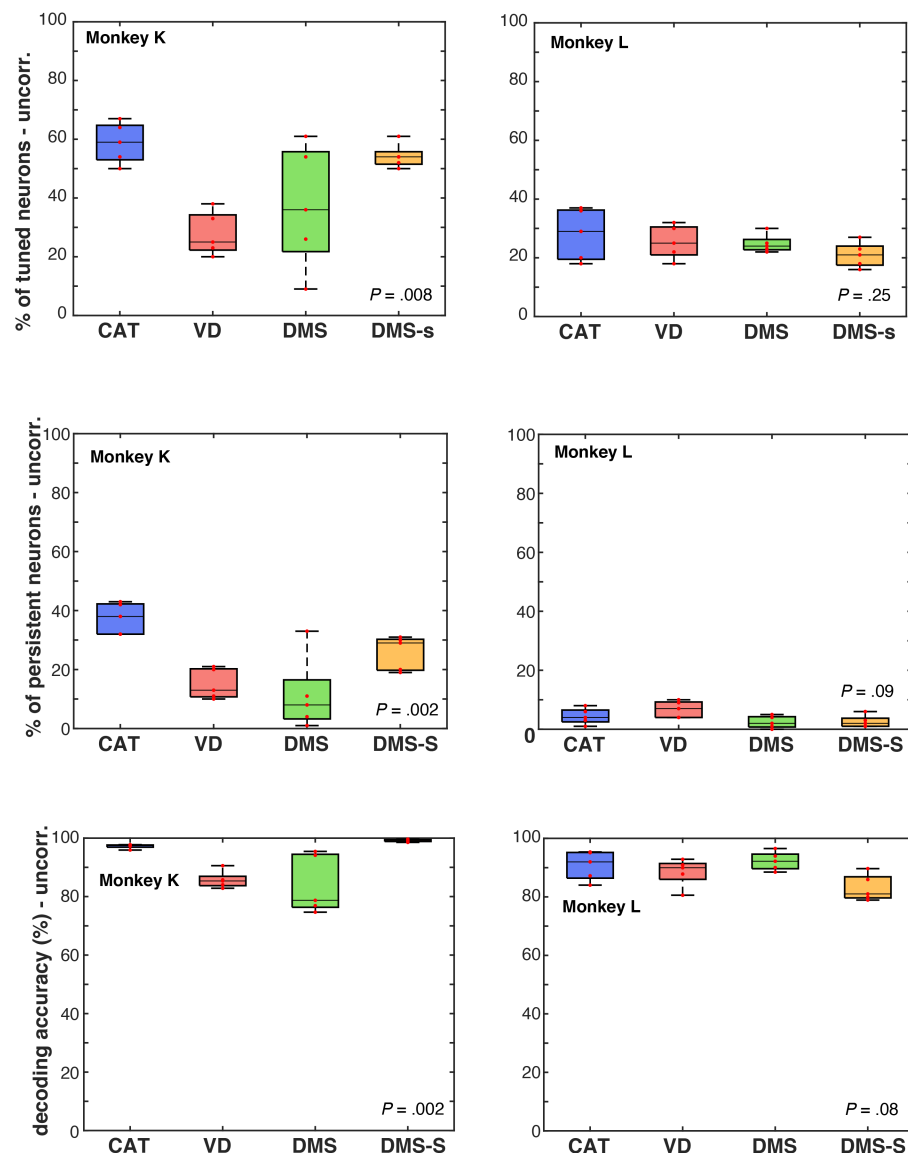
14

Supplementary Figures

Supp. Fig. 1. Single neuron examples for monkey L. Example single neuron spiking activity during the performance of each task, averaged over trials, for monkey L. Trials are separated based on whether target 1 or target 2 needed to be selected on this trial. This selection depended on the cognitive task. Shaded area shows significant tuning during the delay epoch of each task, when no stimuli is on the screen. Error bars are SEM.

15

Supp. Fig. 2. Capturing uninstructed movements. (**A**) View of the experimental setup with a head-free monkey performing a task on the touchscreen. The position of a video camera and a head-free eye-tracker are indicated. (**B**) Video tracking of macaque body movements during task performance. Various cameras and analyses techniques were used to quantify movements of 9 body parts. (**C**) Average eye (top) and head (bottom) traces during the delay of an example session in monkey K. Traces are separated based on decision to later select the star or the target. The difference between these two traces indicates uninstructed movements aligned with a critical task variable (i.e. the decision). The size of those spatial biases, calculated in degrees of visual angle for the eyes and in cm for the head, was used in the regression model to control for those movements. (**D**) Same as in (C), but for monkey L. Monkey L had much fewer uninstructed movements aligned to task variables.

Supp. Fig. 3. Task-aligned uninstructed movements correlating with neural metrics. Correlations between eye bias or head bias estimates, as detailed in **Supp Fig. 2**, and the three neural metrics reported: % of tuned neurons (left column), % of persistent neurons (middle), and decoding accuracy (right). Note the strong biases in monkey K that vary across tasks (color legend), and correlate with neural metrics. Monkey L, in comparison, didn't exhibit such biases or correlations with neural metrics.

Supp. Fig. 4. Uncorrected comparisons across tasks. Proportion of tuned neurons (top), of persistent firing neurons (middle), and decoding accuracy (bottom) when uncorrected for uninstructed movements aligned to task variables. Monkey K presented a large amount of uninstructed movements that biased tuning estimates across tasks (see **Supp. Fig. 2, 3**). Conventions as in **Figure 2D-F**.